

An Experimental Study on Coupled Balancing Tasks Between Human Subjects and Artificial Controllers

Shigeki Matsumoto, Katsutoshi Yoshida and Atsushi Higeta

Department of Mechanical and Intelligent Engineering, Utsunomiya University,
Yoto 7-1-2, Utsunomiya, Tochigi 321-8585, Japan
E-Mail: matsumoto@katzlab.jp

Abstract

Coupled human balancing tasks, performed by a pair of artificial controllers and a pair of human subjects, have been studied by the present authors based on the coupled inverted pendula (CIP) model. On the contrary, in this paper, we examine another type of combination, the artificial controller and the human subject. We experimentally estimate Lyapunov and sub-Lyapunov exponents of balancing errors of the system of human subject and artificial controller, in which the human subject is in cooperation with the artificial controller having several different feedback gains. The result implies that the human subject seems to try to make the artificial controller minimally or neutrally stable.

1 Introduction

Competitive and cooperative dynamics can arise when multiple agents such as humans and robots share common resources and environment[1, 2, 3]. Seeking a simpler description of such dynamics, we have already proposed the coupled inverted pendula (CIP) model as shown in Fig.1. The CIP model consists of two inverted pendulums independently stabilized whose tips are mechanically linked by a rigid rod [4, 5]. As discussed in the studies above [3], the CIP model can produce nonlinear dynamics comparable to interspecific competition of ecosystem and is expected to provide one of the simplest description of the competitive and cooperative dynamics of the coupled agents [4]. Furthermore, in our recent studies [6, 7], replacing the feedback controller of the CIP model with the natural human balancing tasks, we have made a comparison between the cooperative balancing dynamics produced by the pair of two human subjects and that by the pair of two artificial controllers.

The artificial controller in our studies was composed by a delayed state feedback controller with a randomly fluctuated gain, which was proposed by Cebrara, Bormann and Milton[8, 9]. They showed numerically and experimentally that intermittent behavior typical of the human balancing tasks can precisely be simulated based on the minimally stable design of the controller[8, 9]. In this context, we also investigated in a stochastic manner that the minimally stable condition in the sense of Lyapunov exponents can be explained by a trade-off be-

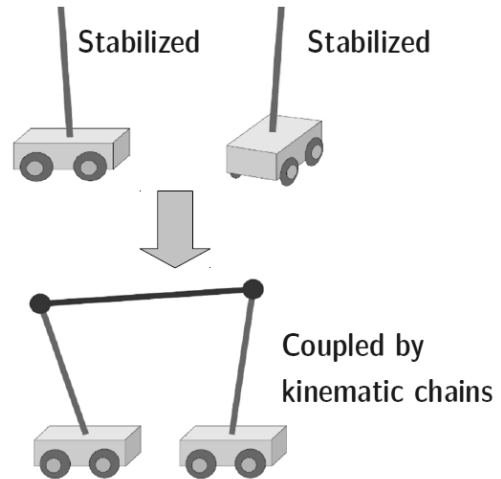


Fig. 1: CIP model.

tween maximal robustness and minimal phase-shift from the disturbance to the second moments[10]. However, this study examined the single balancing case only, where each agent performs its own balancing task independently. Thus, it seems that little is known about the design principles of the coupled balancing between the human subject and the artificial controller.

In this paper, we experimentally study how human subjects tune their control properties when playing balancing tasks in cooperation with a given artificial controller having several different specifications. To this end, we develop an experimental system composed by a numerical simulator of the CIP whose control input can be connected with the human manipulation by mice and/or the artificial controller. The proposed system can also be used for the single balancing experiment by removing the constraint between the tips of pendulums. Based on this system, we conduct three types of experiment: the single human balancing, the single artificial balancing, and the coupled balancing between a human subject and an artificial controller. Then, in order to evaluate their dynamic stabilities, we calculate Lyapunov exponents and sub-Lyapunov exponents of their balancing errors. As a result, it will be shown that the human subjects in cooperation with the artificial controller tends to make the artificial controller minimally or neutrally stable.

Table 1: List of state vectors

	Single balance	Coupled balance
Human agent	$\Delta \mathbf{x}_H = (\Delta x_H, \Delta \dot{x}_H)^T$ where $\Delta x_H := x_H^t - x_H^c$	$\Delta \mathbf{X}_H = (\Delta X_H, \Delta \dot{X}_H)^T$ where $\Delta X_H := X^t - X_H^c$
Artificial agent	$\Delta \mathbf{x}_A = (\Delta x_A, \Delta \dot{x}_A)^T$ where $\Delta x_A := x_A^t - x_A^c$	$\Delta \mathbf{X}_A = (\Delta X_A, \Delta \dot{X}_A)^T$ where $\Delta X_A := X^t + l - X_A^c$
Total dynamics		$\Delta \mathbf{X} = (\Delta X_H, \Delta \dot{X}_H, \Delta X_A, \Delta \dot{X}_A)^T$

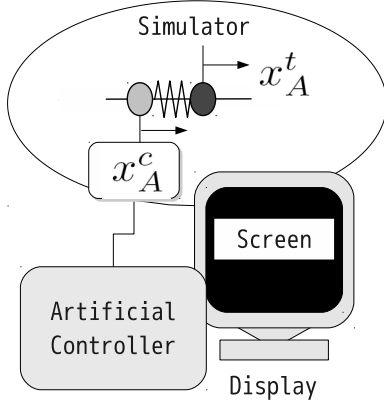


Fig. 2: Single balance control system with an artificial agent.

2 Single balancing tasks

Firstly, we describe the basic mechanism of the artificial controller used in this paper. It is known that single human stick balancing tasks and their scaling properties can be accurately modeled as an inverted pendulum with a time-delayed feedback of random gain in the following form [8, 9]:

$$\ddot{\theta} + \gamma \dot{\theta} - \alpha \sin \theta + \beta R(t) \theta(t - \tau) = 0 \quad (1)$$

where τ is a time delay representing the latency of neural reflexes in human balancing tasks and $R(t) = 1 + \nu w_t(t)$ is a random feedback gain, $w_t(t)$ is standard Gaussian white noise and ν represents the strength of the noise.

Suppose $\theta \approx \Delta x$, $|\Delta x| \ll 1$, we obtain the linearized form of (1):

$$\Delta \ddot{x} + \gamma \Delta \dot{x} - \alpha \Delta x + \beta R(t) \Delta x(t - \tau) = 0 \quad (2)$$

where $\Delta x := x^t(t) - x^c(t)$ the relative displacement that is regarded as an approximation of θ where x^t and x^c is an absolute position of the upper and lower end of the stick respectively. In the following, we refer to Δx as a balancing error and also refer to the upper and lower end of the stick as a target and a cart respectively.

2.1 Artificial control

We develop a balance control system with a single artificial agent as schematically shown in Fig.2. The simu-

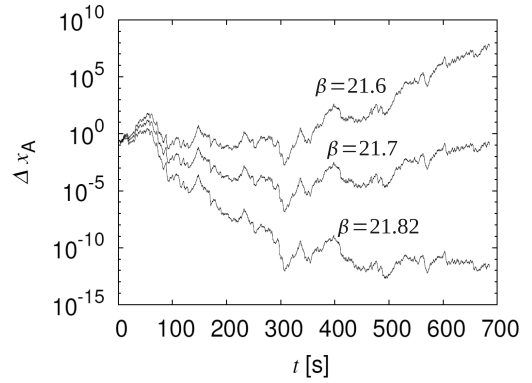


Fig. 3: Sample paths of the balancing error $\Delta x_A(t)$.

lator is based on the linearized model (2). The target x_A^t is repelled from the cart x_A^c by a linear spring with the negative coefficient $-\alpha < 0$ that simulates the gravity force in the original inverted pendulum. Then, we define the artificial controller generating a control input that makes the cart track the target, given by

$$\begin{cases} \ddot{x}_A^t + \gamma \dot{x}_A^t - \alpha \Delta x_A = 0, \\ \ddot{x}_A^c + \gamma \dot{x}_A^c = \beta R(t) \Delta x_A(t - \tau), \\ \Delta x_A := x_A^t - x_A^c \end{cases} \quad (3)$$

where Δx_A is the balancing error of this system and x_A^t , x_A^c are the absolute positions of the target and the cart respectively. In the following, we assume $\gamma = 6$, $\alpha = 22$, $\nu = 2$ and $\tau = 0.1$.

For convenience of reference, Table 1 lists the notation of state vectors used in this paper including Δx_A , x_A^t and x_A^c above. That is, the lower case and upper case of vectors represents the single and coupled balance respectively, and subscripts H and A represents the human and artificial agents respectively.

Fig.3 shows sample paths obtained from (3) subjected to a common sample of the noise $w_t(t)$. It appears that the state $\Delta x_A(t)$ diverges for the gain $\beta = 21.6$ and converges for the gain $\beta = 21.8$. On the other hand, near half point $\beta = 21.72$, the bounded state wandering around

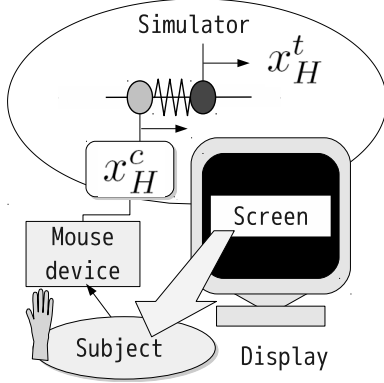


Fig. 4: Single balance control system with a human agent.

$|\Delta x_A(t)| \approx 10^0$ appears. Therefore, not surprisingly, it is confirmed that stabilities of the single balance control system with an artificial agent directly depends on the feedback gain β .

2.2 Human control

We also develop a balance control system with a single human agent as schematically shown in Fig.4. Watching the computer screen displaying a simulated motion of the linearized inverted pendulum, the subject manipulates the displacement of cart x_H^c by mice. In this system, the subject can perform a balancing task, manipulating the cart x_H^c to make it track the target repelling from the cart. To achieve this, we replace the second equation of (3) with the human manipulation as follows.

$$\begin{cases} \ddot{x}_H^t + \gamma \dot{x}_H^t - \alpha \Delta x_H = 0, \\ x_H^c := (\text{manipulation by a human subject}), \\ \Delta x_H := x_H^t - x_H^c \end{cases} \quad (4)$$

where Δx_H is the balancing error and x_H^c is a manipulation by a human subject.

Based on this system, we conduct the experiment to measure the time series of x_H^t and x_H^c in (4), for 10 subjects who were healthy males in their early twenties. The subjects were first instructed in how to operate of the measurement system, the number of trials to be performed, the initial configuration of the target model, and the time interval of trial.

In the actual trial, they began the operation upon hearing a signal and attempted to maintain the balance for 60 sec. If a target or cart left the screen in less than 60 sec, the trial was repeated. After completing the 10 trials, the measurements were over.

Fig.5 shows a typical time series of the balancing error $\Delta x_H(t)$ produced by a human subject. It appeared that amplitudes of the balancing error $\Delta x_H(t)$ rapidly decreases in about 2s to drop into some stationary state fluctuated around $\Delta x_H(t) = 0$ with small amplitudes.

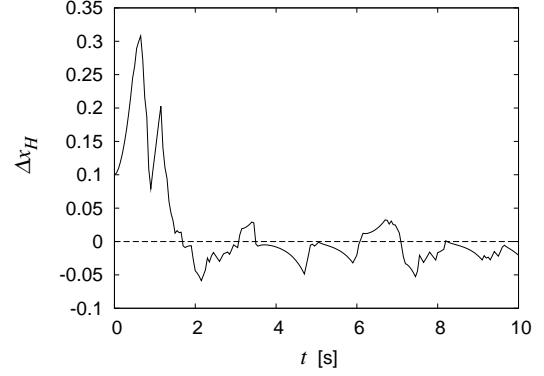


Fig. 5: Time series of the balancing error $\Delta x_H(t)$.

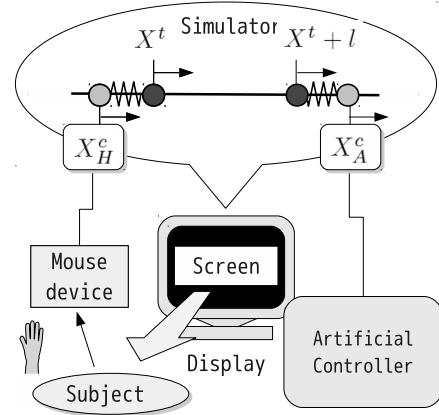


Fig. 6: Coupled balance control system with the human and artificial agents.

3 Coupled balancing tasks

The main interest of this paper is to combine the artificial and human balance control systems discussed in Chapter 2 into a coupled balance control system with the human and artificial agents as shown in Fig.6. In this coupled balance, one of the carts is controlled by the artificial controller as was in Section 2.1 and the other cart is manipulated by the human subject as was in Section 2.2. The desired system can be obtained by

$$\begin{cases} \ddot{X}^t + \gamma \dot{X}^t - \frac{\alpha}{2} (\Delta X_H + \Delta X_A) = 0, \\ X_H^c := (\text{manipulation of human subjects}), \\ \ddot{X}_A^c + \gamma \dot{X}_A^c = \beta R(t) \Delta X_A(t - \tau), \\ \Delta X_H := X^t - X_H^c, \\ \Delta X_A := X^{t+l} - X_A^c \end{cases} \quad (5)$$

where ΔX_H , ΔX_A are balancing errors of the human subject and artificial controller respectively, l is a length of link, X_H^c is a manipulation of the human subject, and X_A^c is an output of the artificial controller defined by the third equation. In the following, we assume $\gamma = 6$, $\alpha = 22$, $l = 1$, $\nu = 2$ and $\tau = 0.1$.

It is noteworthy that in this system, the artificial agent

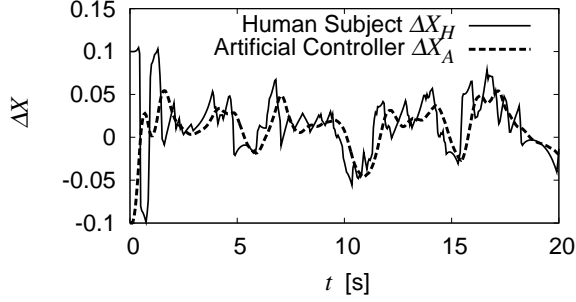


Fig. 7: Balancing error ΔX_H and ΔX_A for $\beta = 23$.

can feedback its own state ΔX_A only, while the human subject can see movements of the artificial partner as well as his own movements.

Following this setup, we conduct the experiment to measure the time series of X^t , X_H^c and x_A^c in (5), for the same subjects as was in Section 2.2 (10 healthy males in their early twenties). However, unlike the experiment in Section 2.2, we have a control parameter β in this coupled experiment, so that in order to examine the effect of β , the value of β is updated in a certain set of trials.

The subjects were first instructed in how to operate of the measurement system, the number of trials to be performed, the initial configuration of the target model, and the time interval of trial. In the actual trial, they began the operation upon hearing a signal and attempted to maintain the balance for 60 sec. If the targets or carts left the screen in less than 60 sec, the trial was repeated. After the 10 trials, the value of feedback gain is updated to be less from 23 to 17 at regular intervals. After completing the 40 trials the measurements were over.

Fig.7 and Fig.8 show typical time series of the balancing errors for $\beta = 23$ and for $\beta = 17$ respectively. The solid line represents a balancing error of the human subject ΔX_H and the dashed line represents that of the artificial controller ΔX_A .

In contrast to the single artificial balance shown in Fig.3 where the stability of $\Delta x_A(t)$ depends on the feedback gain β , it seems that no significant dependency on β can be found for the coupled balance shown in Fig.7 and Fig.8. That is, it seems that there is no significant change of stability of ΔX_H and ΔX_A around $\Delta X = 0$ between the different conditions $\beta = 23$ and $\beta = 17$.

4 Stability of coupled balancing tasks

4.1 Lyapunov exponents

In order to evaluate dynamic stabilities of the balancing errors listed in Table 1, we employ the Lyapunov exponents as follows[11].

Consider a n -dimensional dynamical system:

$$\dot{\mathbf{x}}(t) = \mathbf{f}(\mathbf{x}(t)) \quad \mathbf{x}(0) = \mathbf{x}_0 \quad (6)$$

and its linearized system:

$$\dot{\boldsymbol{\xi}}(t) = J(\mathbf{x}(t))\boldsymbol{\xi}(t), \quad \boldsymbol{\xi}(0) = \boldsymbol{\xi}_0 \quad (7)$$

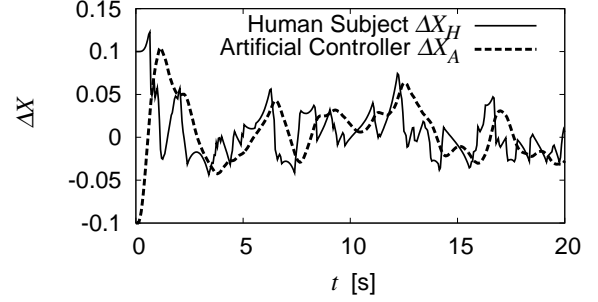


Fig. 8: Balancing error ΔX_H and ΔX_A for $\beta = 17$.

where $J(\mathbf{x}) = \partial \mathbf{f} / \partial \mathbf{x}$ is the Jacobian matrix of \mathbf{f} along the orbit $\mathbf{x}(t)$. Then, the largest Lyapunov exponent (LLE) of the dynamical system (6) is defined by

$$\lambda(\mathbf{x}) = \max_{\boldsymbol{\xi}_0} \lim_{t \rightarrow \infty} \frac{1}{t} \ln \frac{\|\boldsymbol{\xi}(t)\|}{\|\boldsymbol{\xi}(0)\|} \quad (8)$$

where $\|\cdot\|$ is a norm of vectors. In general, the trajectory $\mathbf{x}(t)$ is stable for $\lambda < 0$, unstable for $\lambda > 0$, and neutrally stable for $\lambda = 0$.

It is noteworthy that the LLE is similar to a real part of the eigenvalue of linear systems in the sense of evaluating dynamic stabilities while their target of evaluation is different. The real part of the eigenvalue of linear systems represents stability of a corresponding equilibrium point. In contrast, the LLE represents local stability of solution trajectories.

When the system equation (6) is explicitly known, one can calculate the LLE $\lambda(\mathbf{x})$ by solving (7) along with (6) numerically. Therefore, in this way, the LLE of the single artificial balance control system, $\lambda(\Delta \mathbf{x}_A)$, can be obtained.

On the contrary, another approach is required for the balance control systems including human agents because their system equation is not explicitly known. For this purpose, we employ an effective method of estimating the LLE from physical time series proposed by Sano and Sawada[11]. In this case, a time series $\mathbf{x}_j = \mathbf{x}(t_0 + (j - 1)\Delta t)$ of the target system is assumed to be known where Δt is a sampling time of measurement. Then, consider a small ball of radius ϵ centred at the orbit point \mathbf{x}_j and find any set of N points $\{\mathbf{x}_{k_i}\}_{i=1}^N$ included in this ball and define the displacement vectors:

$$\begin{cases} \mathbf{y}^i := \mathbf{x}_{k_i} - \mathbf{x}_j, \\ \mathbf{z}^i := \mathbf{x}_{k_{i+1}} - \mathbf{x}_{j+1}, \end{cases} \quad (i = 1, 2, \dots, N). \quad (9)$$

If the radius ϵ is sufficiently small, the evolution of \mathbf{y}^i to \mathbf{z}^i can be represented by

$$\begin{aligned} \mathbf{z}^i &= A_j \mathbf{y}^i, \quad A_j V = C, \\ (V)_{kl} &= \frac{1}{N} \sum_{i=1}^N (\mathbf{y}^i)_k (\mathbf{y}^i)_l, \quad (C)_{kl} = \frac{1}{N} \sum_{i=1}^N (\mathbf{z}^i)_k (\mathbf{y}^i)_l \end{aligned} \quad (10)$$

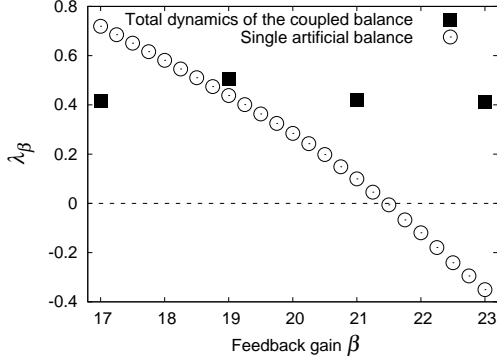


Fig. 9: LLE of the total dynamics of coupled balance and the single artificial balance as functions of the gain β .

where $(\dots)_k$, $(\dots)_{kl}$ denotes the k component of vector and the (k, l) component of matrix respectively. Finally, using the estimated matrix A_j in (10), we can define the LLE of the time series \mathbf{x}_j as

$$\lambda(\mathbf{x}_j) = \max_{\mathbf{u}} \lim_{n \rightarrow \infty} \frac{1}{n\Delta t} \sum_{j=1}^n \ln \frac{\|A_j \mathbf{u}\|}{\|\mathbf{u}\|} \quad (11)$$

where \mathbf{u} is tangent vector at \mathbf{x}_j . In this way, we can obtain the LLE such as $\lambda(\Delta \mathbf{x}_H)$ for the single balance with a human agent, $\lambda(\Delta \mathbf{X})$ for the coupled balance with human and artificial agents. In the same way, it is also possible to obtain the sub-LLE of the human part $\lambda(\Delta \mathbf{X}_H)$ and the artificial part $\lambda(\Delta \mathbf{X}_A)$ of the coupled balance.

In what follows, the LLE were averaged over total 100 data accumulated from 10 subjects to improve statistical reliability.

4.2 LLE of the total dynamics

The black squares in Fig.9 represent the LLE, $\lambda_\beta(\Delta \mathbf{X})$, of the total dynamics of coupled balance between human and artificial agents, and the white circles represent $\lambda_\beta(\Delta \mathbf{x}_A)$ of the single artificial balance, as functions of the feedback gain β .

Since $\lambda_\beta(\Delta \mathbf{x}_A)$ is a monotonically decreasing function of β , it is clear that the stability of the single artificial balancing depends on the feedback gain β . In contrast, as $\lambda_\beta(\Delta \mathbf{X}) \approx 0.4 > 0$ for any β in this graph, it is found that the coupled balance of human and artificial agents is unstable of nearly constant in this domain of β .

Note that the bounded trajectories as shown in Fig.7 and Fig.8 are unstable. As is often in the case of chaotic systems, it is quite possible that the LLE of a bounded trajectory takes positive value. The LLE represents a strength of a fluctuation of the trajectory in this case. The balancing error of the total dynamics $\Delta \mathbf{X}$ exhibits the largest fluctuation of the trajectory among three types of balancing errors of the coupled balance listed in Table 1.

As for the coupled balance, since β represents the feedback gain of the artificial part, not of the human part, the result implies that the nearly constant instability of the

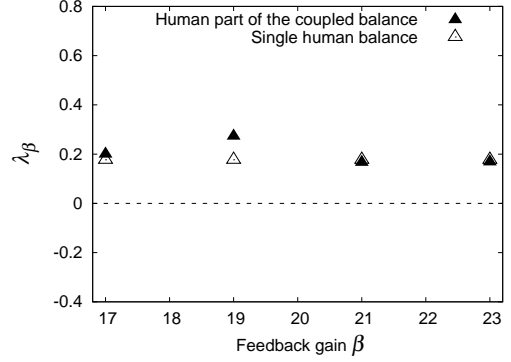


Fig. 10: Sub-LLE of the human part of the coupled balance and LLE of the single human balance as functions of the gain β .

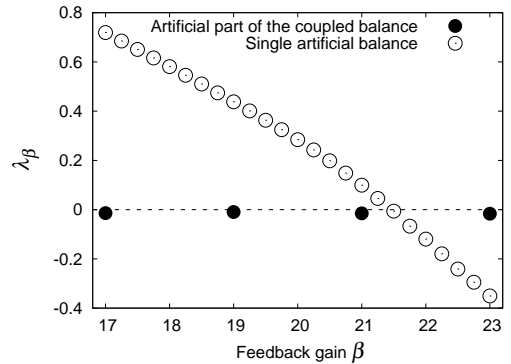


Fig. 11: Sub-LLE of the artificial part of the coupled balance and LLE of the single artificial balance as functions of the gain β .

coupled balance found in Fig.9 is possibly produced by the human part. In other words, it seems that the human part may adjust itself to make the total stability of the coupled balance nearly constant. This feature can also be found in Fig.7 and Fig.8 where the different values of β does not cause big changes in the time responses of the coupled balance.

4.3 Sub-LLE of the human part

The black triangles in Fig.10 represent the LLE, $\lambda_\beta(\Delta \mathbf{X}_H)$, of the human part of the coupled balance as a function of β , and the white triangles represent the LLE, $\lambda_\beta(\Delta \mathbf{x}_H)$ of the single human balance.

It appears that both $\lambda_\beta(\Delta \mathbf{X}_H)$ and $\lambda_\beta(\Delta \mathbf{x}_H)$ take nearly constant positive values around $\lambda_\beta \approx 0.2 > 0$, and the balancing error of the human part $\Delta \mathbf{X}_H$ exhibits the second largest fluctuation of the trajectory among three types of balancing errors of the coupled balance listed in Table 1. This means that the human balancing dynamics exhibits nearly constant instability independently of existence of coupling and of the feedback gain of the artificial part.

4.4 Sub-LLE of the artificial part

The black circles in Fig.11 represent the LLE, $\lambda_\beta(\Delta \mathbf{X}_A)$, of the artificial part of the coupled balance,

and the white circles represent $\lambda_\beta(\Delta\mathbf{x}_A)$ of the single artificial balance, as functions of the feedback gain β .

As was mentioned in Section 4.2 for the single balance, the LLE, $\lambda_\beta(\Delta\mathbf{x}_A)$, is a monotonically decreasing function of β , showing that the stability of the single artificial balancing depends on the feedback gain β .

In contrast, it is clear from the result on $\lambda_\beta(\Delta\mathbf{X}_A)$ that the artificial part of the coupled balance maintains nearly a constant value about 0 of the LLE, and the balancing error of the artificial part $\Delta\mathbf{X}_A$ exhibits the smallest fluctuation of the trajectory among three types of balancing errors of the coupled balance listed in Table 1. This result shows that human subject seems to try to make the artificial controller minimally or neutrally stable.

5 Conclusion

We have experimentally studied how human agents tune their control properties when playing balancing tasks in cooperation with a given artificial controller having several different specifications of feedback gain β . To this end, we conducted the experiment to measure the time responses of the balancing errors in the single human balance, the single artificial balance, and the coupled balance between a human agent and an artificial agent. We then calculated the largest Lyapunov exponent (LLE) of the balancing errors in order to evaluate their stabilities and obtained the following results.

- The stability of the single artificial balance monotonically depends on the feedback gain β .
- In contrast, the total dynamics of the coupled balance between the human and artificial agents exhibits instability nearly constant with β .
- The human agent always exhibits nearly constant instability with β in both cases of the single balance and the coupled balance.
- The artificial part in the coupled balance maintains neutrally stable state independent of β .

From the above result, it can be concluded that the human balancing agent in cooperation with the artificial agent may adjust itself to make the artificial partner minimally or neutrally stable independently of the feedback gain of the artificial partner.

Acknowledgement

We wish to express our gratitude to the members of the System Dynamics Laboratory of the Faculty of Engineering at Utsunomiya University for their participation and cooperation as subjects in this study.

References

- [1] Osumi, H., et al., Cooperative System between a Position-controlled Robot and a Crane with Three Wires, *Distributed Autonomous Robotic Systems*, pp.347-358, 1994.
- [2] Hirata, Y., et al., Handling of a Large Object using Multiple Mobile Robots in Coordination, *Trans. JSME, Series C Vol.67, No.656*, pp.1077-1084, 2001. (in Japanese)
- [3] Sigmund, K. and Hofbauer, J., *Evolutionary Games and Population Dynamics*, Cambridge University Press, 1998.
- [4] Yoshida, K., Yokota, K., and Watanabe, S., A Study on Mechanical System Representation of Competition and Cooperation, *Trans. JSME, Series C Vol.74, No.741*, pp.1311-1316, 2008. (in Japanese)
- [5] Yoshida, K., and Ohta, H., Coupled Inverted Pendula Model of Competition and Cooperation *Journal of System Design and Dynamics*, Vol.2, No.3, pp.727-737, 2008.
- [6] Yoshida, K., Higeta, A., and Watanabe, S., Effects of Mechanical Coupling on the Dynamics of Balancing Tasks, *International Journal of Innovative Computing, Information and Control*, Vol.7, No.4, pp.1661-1674, 2011.
- [7] Higeta, A., Yoshida, K., Watanabe, S., and Nakatsuka, A., Psychological Measurement of Coupled Human Balancing Tasks. *Proceedings of the 2011 IEEE/SICE International Symposium on System Integration*, pp.661-666, No.C9-3(CD-ROM), 2011.
- [8] Cabrera, J. L., and Milton, G. J., On-off intermittency in a Human Balancing Task. *Phys. Rev. Lett.*, Vol.89, No.15, pp.158702:1-4, 2002.
- [9] Bormann, R., Cabrera, J. L., Milton, J. G., and Eulich, C. W., Visuomotor tracking on a computer screen an experimental paradigm to study the dynamics of motor control. *Neurocomputing*, Vol.58, No.60, pp.517-523, 2004.
- [10] Yoshida, K., Toward Stochastic Explanation of Neutrally Stable Delayed Feedback Model of Human Balance Control. *International Journal of Innovative Computing, Information and Control*, Vol.8, No.3(B), pp.2249-2259, 2012.
- [11] Sano, M., and Sawada, Y., Measurement of the Lyapunov Spectrum from a Chaotic Time Series. *Phys. Rev. Lett.*, Vol.55, No.10, pp.1082-1085, 1985.